Electronic Supplementary Material (ESI) for New Journal of Chemistry. This journal is © The Royal Society of Chemistry 2023

Electronic Supplementary Material

A smart portable electrochemical sensor based on electrodeposited ferrocene functionalized multiwalled carbon nanotubes for in vitro and in vivo detection of nicotine in tobacco samples

Zhaohong Su[a,b], Shiyu Hu[b], Yanqun Xu[a], Ju Liu[b], Pengcheng Liang[b], Jiaqi Wang[b], Qinyi Cao[b], Yi Peng[b], Wei Zhang*[,a], Duoqing Fan*[,a]

[a] Yunnan Key Laboratory of Tobacco Chemistry, R&D Center of China Tobacco Yunnan Industry Co., Ltd. 650231 Kunming, PR China.

[b] College of Chemistry and Materials Science, Hunan Agricultural University, Changsha 410128, PR China.

*Corresponding author. Tel.: +86 871 65869755; Fax: +86 871 65869755.

E–mail address: 13888102860@139.com (Wei Zhang); fanduoqing@sina.com (Duoqing Fan)

Table S1. The impedance fits the values of each component in the circuit diagram

Electrode	Rs/Ω	Rct/Ω	CPE/μF	W/Ω
SPCE	70.56	539.9	0.483	2.80×10^{-3}
MWCNTs/SPCE	72.00	143.9	6.56	2.61×10^{-3}
FC-MWCNTs/SPCE	78.39	64.3	19.3	2.66×10^{-3}

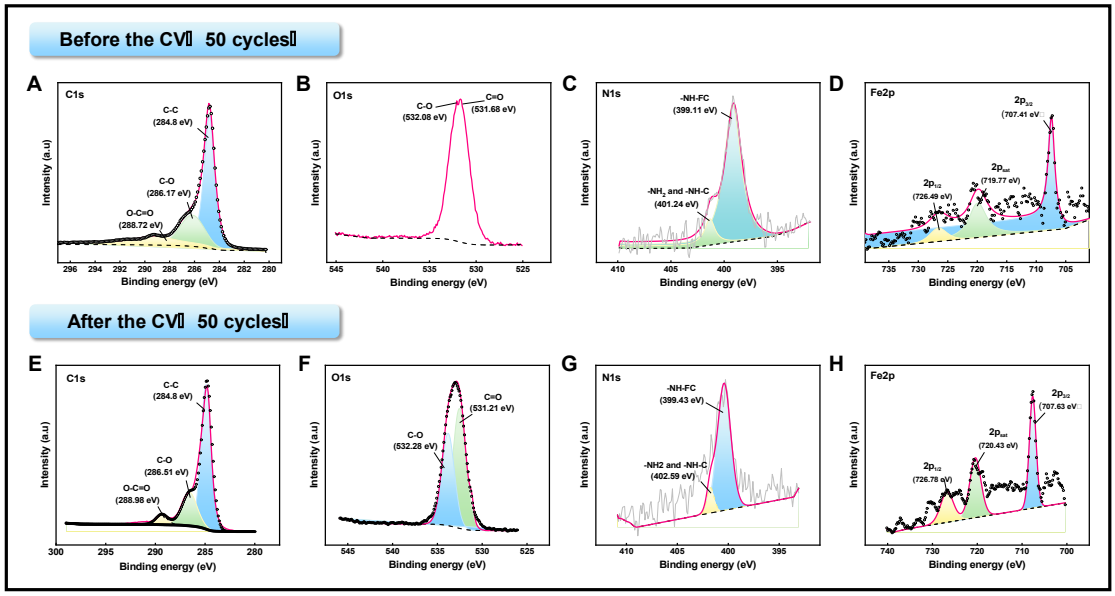

Fig. S1. XPS of FC-MWCNTs/SPCE before (A-D) and after (E-H) 50 cycles of CV in 5.0 mM $[Fe(CN)_6]^{3-/4-}$ + 0.1 M KCl solution.

Table. S2. Composition (atom %) of samples from XPS analysis.

Element	Atomic fraction/% (before cycle)	Atomic fraction/% (after cycle)
C	84.42	83.66
O	13.89	14.77
N	1.45	1.33
Fe	0.24	0.24

XPS was used to characterize the changes of FC-MWCNTs/SPCE after 50 cycles of CV in 5.0 mM $[Fe(CN)_6]^{3-/4-}$ + 0.1 M KCl solution. The C1s spectra can be deconvoluted into 3 bands centered at 284.4eV(C-C) and 286.1eV (C-O), while the peaks at 288.7eV are attributed to O-C=O. The O1s spectrum peaks at C-O (532 eV) and C=O (531.6 eV).Element C and O was mainly provided by carbon nanotubes, and the analysis results were consistent with previous characterization of MWCNTs[1, 2]. The N1s spectra showed the characteristic peaks of ferrocene cross-linked on carbon nanotubes by amide bond : -NH-FC (399.1 eV) and -NH-C- (401.2 eV)[3].What's more, it unfolds into three peaks at 707.4 eV, 719.7 eV, and 725.4 eV (Fig.S1D). 707.4 eV and 725.4 eV correspond to the $2p_{3/2}$, $2p_{1/2}$ orbits of Fe2p, respectively, and the 2psat peak of 719.7 eV corresponds to a shake-up satellite peak characteristic of the Fe^{2+} state[3, 4]. It can also be seen from Table. S2 that the content of Fe element accounts for 0.24%. The results indicated that FC-MWCNTs were successfully synthesized.

The above results show that the material structure of FC-MWCNTs did not change significantly after 50 cycles. The atom% of material elements C and N decreased by 0.76% and 0.12% respectively, the content of O increased by 0.88%, and Fe remained unchanged. The loss of this material in continuous testing was reasonable, and it was also consistent with the result of the gradual reduction of CV in Fig. 4D. All these indicate that FC-MWCNTs/SPCE have good stability.

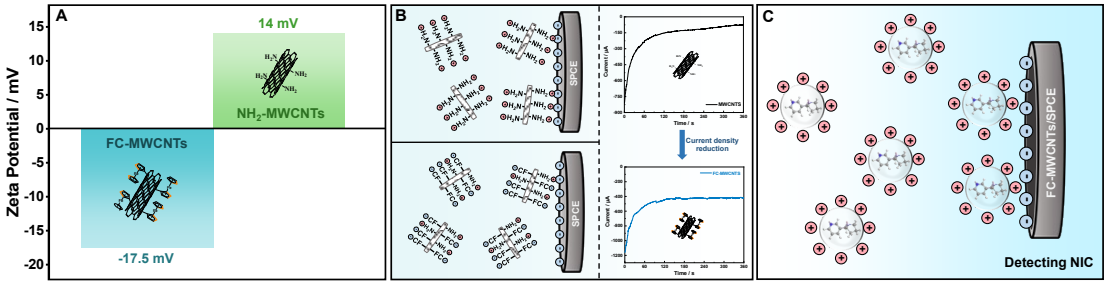

Fig. S2. (A) Average zeta potential of NH_2-MWCNTs and FC-MWCNTs. (B) Electrodeposition diagram of NH_2-MWCNTs and FC-MWCNTs. (C) Schematic diagram of NIC detection by adsorption of FC-MWCNTs.

In order to investigate the function of functional groups on carbon tubes, we did a series of experiments. First of all，-NH_2 plays a bridging role. First, -NH_2 of NH_2-MWCNTs undergoes an amide reaction with -COOH of FC-COOH to produce FC-MWCNTs. Secondly, by comparing the electrodeposition curves of the two materials (Fig. S2B), it was found that the current density of FC-MWCNTs decreased compared with that of MWCNTs during electrodeposition, indicating that after the introduction of negatively charged FC, FC-MWCNTs will repel the negatively charged electrode surface, resulting in a decrease in current density. It is speculated that during the preparation of FC-MWCNTs, FC-COOH can not completely replace -NH_2 of MWCNTs and retained a small part of -NH_2. According to zeta potential analysis (Fig. S2A), Average zeta potential of NH_2-MWCNTs is 14 mV. Therefore, the negative potential energy is used to electrodeposit positively charged -NH_2 onto the surface of the working electrode by applying -1.8 V, thus completing the preparation of FC-

MWCNTs/SPCE (Fig. S2B). According to the literature[5], NIC is positively charged in PBS (pH=7.4). Average zeta potential of FC-MWCNTs is -17.5 mV (Fig. S2A), indicating that the electrode modified with FC-MWCNTs can adsorb positively charged NIC to the electrode surface for NIC detection (Fig. S2C).

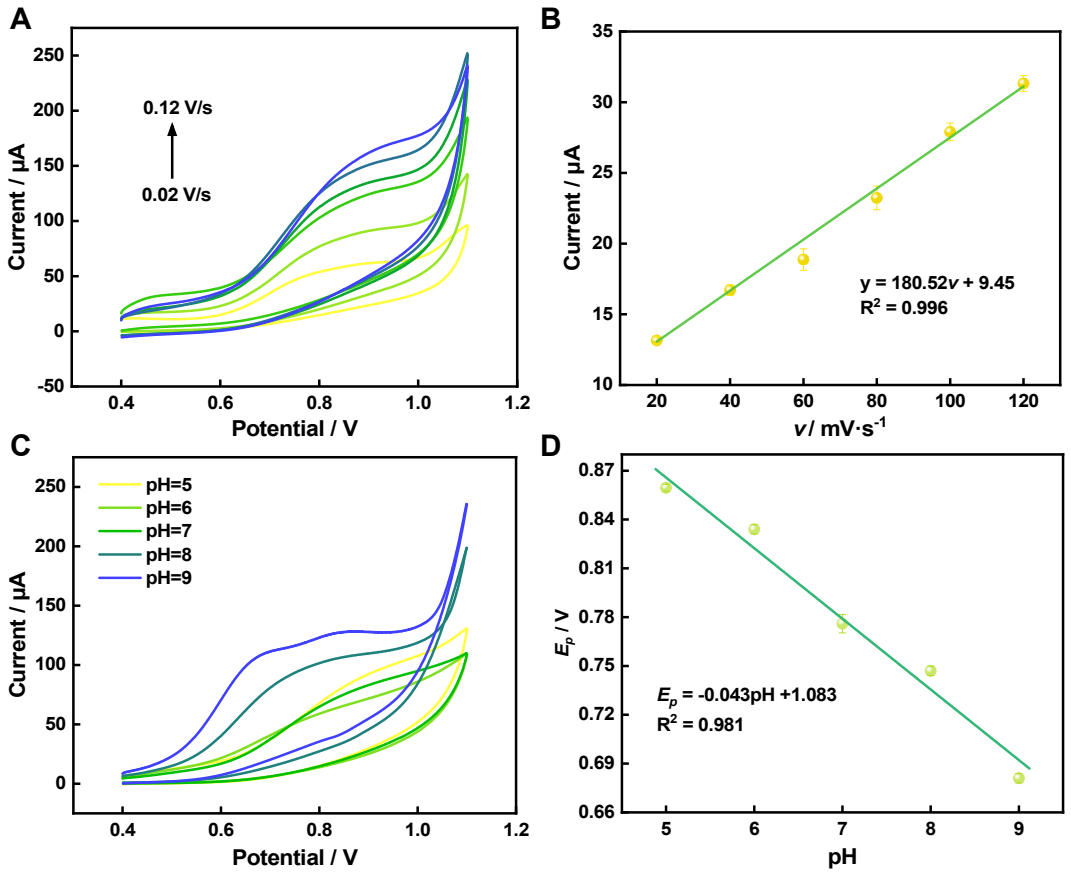

Fig. S3 (A) CV of FC-MWCNTs/SPCE in 0.1 M PBS containing 100 μM NIC (pH =7.4) at different scanning rate. (B) Relation diagram between response current and scanning rate. (C) CV of FC-MWCNTs/SPCE in 0.1 M PBS (pH = 5, 6, 7, 8, 9) containing 100 μM NIC. (D) Diagram of the relationship between peak potential and pH.

The electrochemical behavior of NIC detected by FC-MWCNTs/SPCE was studied. Fig. S3A shows that I_{NIC} increases with the increase of the scanning rate. During the anodic scanning process, the NIC on the surface of the modified electrode begins to oxidize at 0.65 V, and the potential of the NIC appears positive shift. NIC has no voltammetric response during the cathodic scanning process, so it is speculated that the oxidation of NIC on the sensor is irreversible. Fig. S3B shows the linear relationship between the oxidation peak current (I_{pa}) and scanning rate (v) of NIC: $I_{pa} = 180.52v + 9.45$ ($R^2 = 0.996$), it indicates that NIC detection by modified electrode is an adsorption control process.

CV was used to study the effect of pH (5.0-9.0) of PBS on NIC current response (Fig. S3C). It can be seen that with the increase of pH, the peak potential moves slightly in the negative direction, indicating that protons participate in the electrode reaction. The relationship of oxidation peak potential (E_p) with pH is shown in the Fig.

S3D: E_p = -0.043pH + 1.083 (R^2=0.981). The slope is 0.043 V/pH, closes to the theoretical value of 0.059V/pH. This shows that the ratio of electrons and protons involved in the electrochemical reaction is 1:1. Additionally, the oxidation peak potentials (E) shifted with the natural logarithm of scan rate (ln v), and the linear regression equation is E (V) = 0.0212 ln v + 0.7823 (R^2 = 0.98). For irreversible reactions controlled by adsorption, the Laviron equation should be followed[6] :

$$E = E_0 + \frac{RT}{\alpha nF}\ln\frac{RTk_0}{\alpha nF} - \frac{RT}{\alpha nF}\ln v$$

the electrons transfer number (n) and transfer coefficient (α) were calculated to be 2.4 (≈2) and 0.50 from the slope of E vs. ln$v$. Therefore, the oxidation reaction of NIC at FC-MWCNTs is a two-electron and two-proton process (Fig.S4C), which is consistent with previous reports [7, 8].

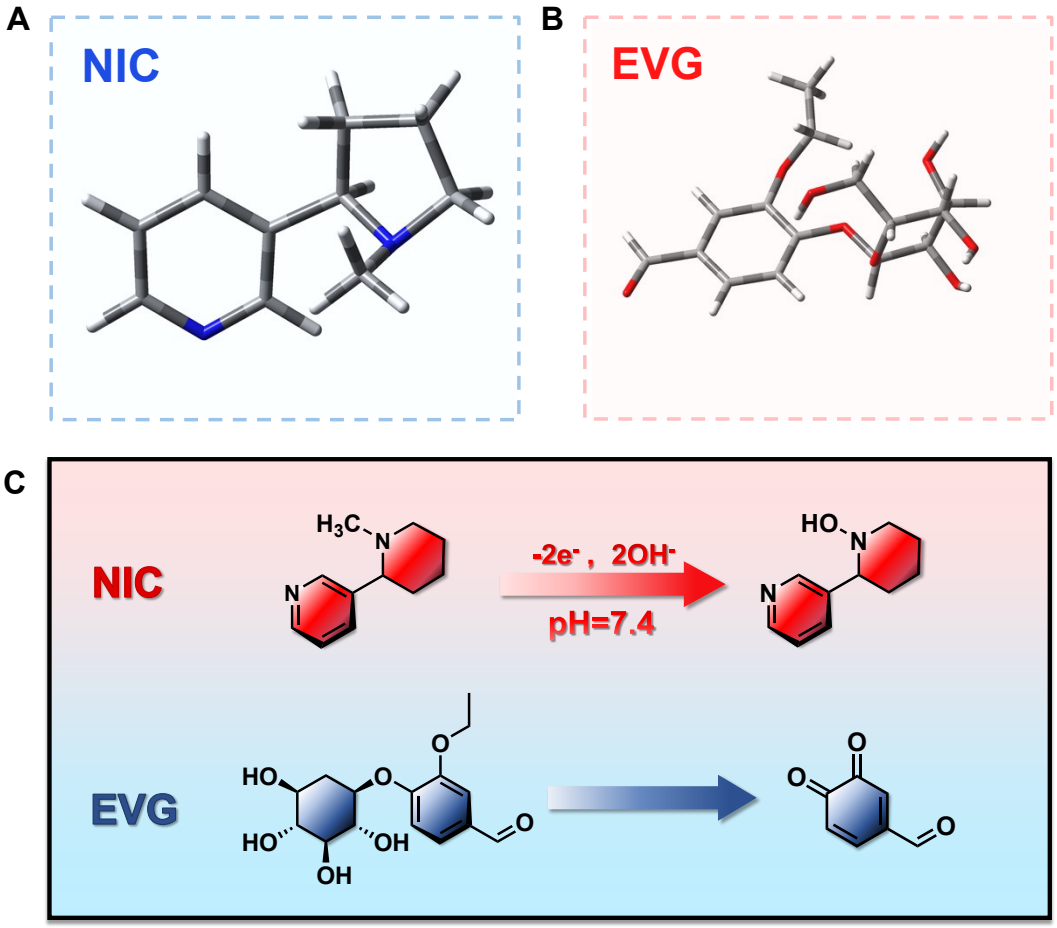

Fig. S4. Structural optimization of NIC (A) and EVG (B). (C) Possible mechanism of electrochemical oxidation of NIC and EVG.

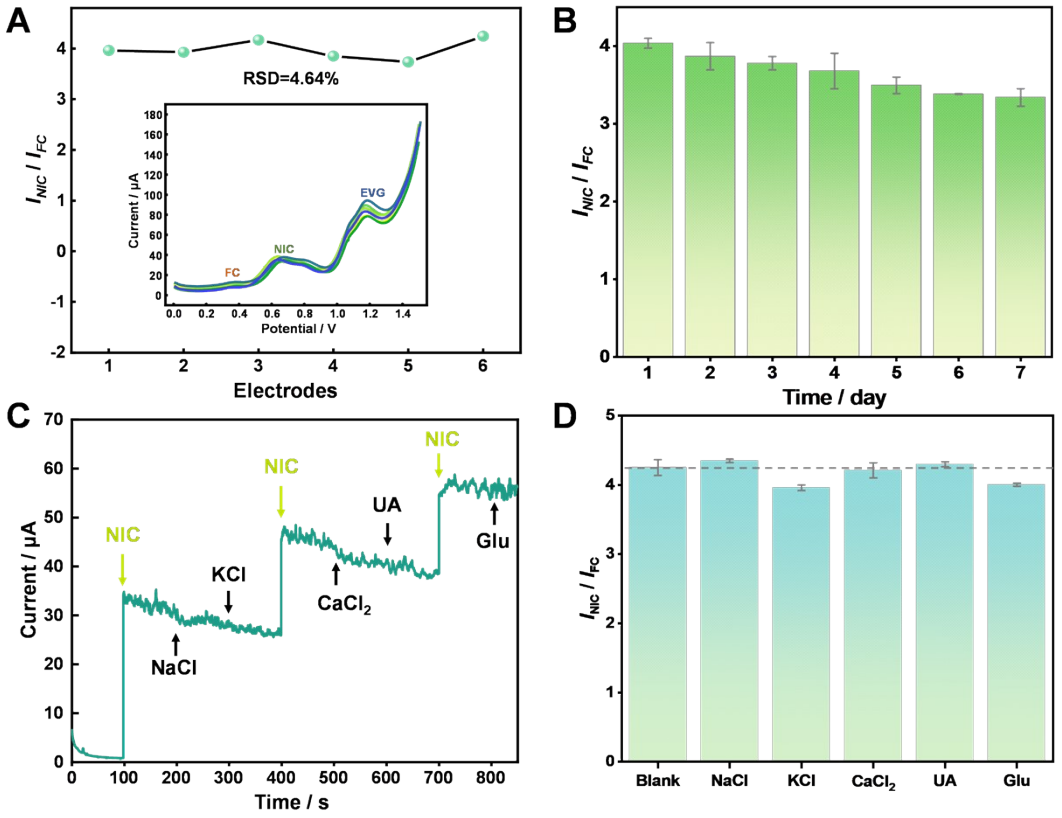

Fig. S5. (A) DPV ratio currents of six FC-MWCNT/SPCE in 0.1M PBS (pH=7.4) containing 100 μmol/L NIC and 100 μmol/L EVG. (B) DPV ratio current changes of FC-MWCNTs/SPCE from 1 day to 7 day in 0.1M PBS (pH=7.4) containing 100 μmol/L NIC and 100 μmol/L EVG. (C) Chronoamperometric curve of FC-MWCNTs/SPCE at 0.85 V in 0.1 M PBS (pH =7.4) with the addition of 100 μM NIC and 1000 μM different interferences. (D) DPV ratio currents of FC-MWCNT/SPCE in 0.1 M PBS (pH =7.4) with the addition of 100 μM NIC and 1000 μM different interferences..

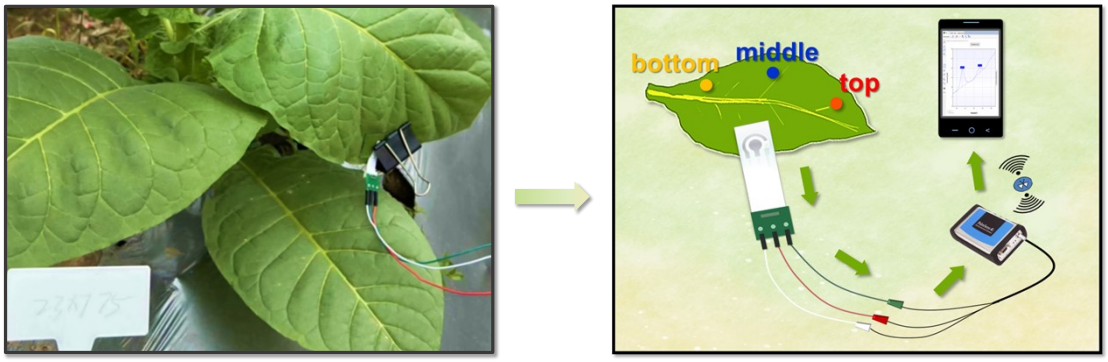

Fig. S6. In vivo testing of two types of tobacco (23×775 and 23×778) at Ningxiang Tobacco Base.

Table S3. In vivo testing of NIC in tobacco leaves

Breed	Top/μM	Middle/μM	Bottom/μM
775	8.415	8.407	8.409
778	8.407	8.410	8.407

References (only for Supporting Information)

1. C. Abate, G. Neri, A. Scala, P. G. Mineo, E. Fazio, A. Mazzaglia, A. Fragoso, O. Giuffrè, C. Foti and A. Piperno, *ACS Appl. Nano Mater.*, 2023, **6**, 17187–17195.
2. B. R. Strohmeier, J. D. Piasecki, K. L. Bunker, J. L. Sturgeon, B. A. Stitch and J. P. Marquis, *Microsc. Microanal.*, 2010, **16**, 442-443.
3. G. A. M. Ali, E. Megiel, P. Cieciórski, M. R. Thalji, J. Romański, H. Algarni and K. F. Chong, *J. Mol. Liq.*, 2020, **318**.
4. X. Niu, X. Yang, Z. Mo, R. Guo, N. Liu, P. Zhao, Z. Liu and M. Ouyang, *Electrochim. Acta*, 2019, **297**, 650-659.
5. Z. Liang, S. Hu, Y. Peng, C. Cheng, J. Luo, L. Yang, M. Yang, X. Yu, Y. Zhao and Z. Su, *IEEE Sensors Journal*, 2024, **24**, 71-77.
6. E. Laviron, *J. Electroanal. Chem.* , **52**, 355-393.
7. E. Mehmeti, T. Kilic, C. Laur and S. Carrara, *Microchem. J.*, 2020, **158**, 105155.
8. J. Rajendran, A. K. Sundramoorthy, D. Ganapathy, R. Atchudan, M. A. Habila and D. Nallaswamy, *J. Hazard. Mater.*, 2022, **440**, 129705.